

High Efficiency Resonant dc/dc Converter Utilizing a Resistance Compression Network

Wardah Inam, Khurram K. Afridi and David J. Perreault
 Department of Electrical Engineering and Computer Science
 Massachusetts Institute of Technology
 Cambridge, Massachusetts 02139

Abstract—This paper presents a new topology for a high efficiency dc/dc resonant power converter that utilizes a resistance compression network to provide simultaneous zero voltage switching and near zero current switching across a wide range of input voltage, output voltage and power levels. The resistance compression network (RCN) maintains desired current waveforms over a wide range of voltage operating conditions. The use of on/off control in conjunction with narrowband frequency control enables high efficiency to be maintained across a wide range of power levels. The converter implementation provides galvanic isolation and enables large (greater than 1:10) voltage conversion ratios, making the system suitable for large step-up conversion in applications such as distributed photovoltaic converters. Experimental results from a 200 W prototype operating at 500 kHz show that over 95% efficiency is maintained across an input voltage range of 25 V to 40 V with an output voltage of 400 V. It is also shown that the converter operates very efficiently over a wide output voltage range of 250 V to 400 V, and a wide output power range of 20 W to 200 W. These experimental results demonstrate the effectiveness of the proposed design.

I. INTRODUCTION

High-voltage-gain dc/dc converters are found in a variety of applications. For example, to connect photovoltaic panels to the grid, interface circuitry is needed. Some architectures for this purpose incorporate dc/dc converters to boost voltage of individual photovoltaic panels to a high dc-link voltage, with follow-on electronics for converting dc to ac (e.g., [1], [2]). The step-up dc/dc converter is a critical part of this system, and must operate efficiently for a large voltage step-up and for a wide voltage range (e.g., at the converter input and/or output depending upon the system). Furthermore, to be compact it must operate at high switching frequencies.

In conventional hard-switched power converters, the overlap of current and voltage is large during switching, resulting in significant power loss, especially at high frequencies. Soft switched resonant converter topologies providing zero voltage switching (ZVS) or zero current switching (ZCS) can greatly reduce loss at the switching transitions, enabling high efficiency at high frequencies (e.g., [3], [4]). Unfortunately, while many soft-switched resonant designs achieve excellent performance for nominal operating conditions, performance can degrade quickly with variation in input and output voltages and power levels.

Limitations on the efficient operating range of resonant converters are tied to both converter structure and control. Numerous control techniques are possible for compensating

variations in input voltage, output voltage, and power level. These include frequency control [3], [4], phase-shift PWM control [5], asymmetric duty cycle PWM control [6], and on-off or burst control [7]. Each of these control techniques in conjunction with conventional resonant tank structures imposes significant design limits. For example, the conventional half-bridge Series Resonant Converter (SRC) [4] requires wide-band frequency variation to control the power when output load or input voltage varies such that the magnetics cannot be optimally designed. Furthermore, to maintain zero-voltage switching the frequency must increase to reduce power, hurting the efficiency at light load. For a full-bridge version of the SRC, phase shift control can be used to control the power and reject conversion ratio variations (e.g., [5]). However, this results in asymmetrical current levels in the switches at the switching instants, with the switches in the leading leg turning off at high currents. The effective impedance of the rectifier in a resonant converter also often causes challenges, as it varies with operating conditions.

This paper introduces a new high efficiency resonant dc/dc converter topology, the Resistance Compression Network (RCN) converter, which seeks to overcome the above-mentioned challenges. This converter operates with simultaneous zero voltage switching (ZVS) and near zero current switching (ZCS) across a wide range of input voltage, output voltage and power levels, resulting in low switching losses.

The remainder of this paper is organized as follows: Section II describes the topology and control of the proposed RCN dc/dc converter. The converter is analyzed and methodology for its design is presented in section III. Section IV describes the design and implementation of a prototype RCN dc/dc converter. The experimental results from this prototype are presented and discussed in section V. Finally, section VI summarizes the conclusion of the paper.

II. RCN CONVERTER TOPOLOGY AND CONTROL

The dc/dc converter proposed here consists of an inversion stage, a transformation stage and a rectification stage, as shown in Fig. 1. The inversion and rectification stages use standard designs. However, the transformation stage and the control of the converter are new. The topology of the proposed Resistance Compression Network (RCN) converter is shown in Fig. 2. The converter as shown is designed to step-up voltage. The transformation stage consists of a matching network, a

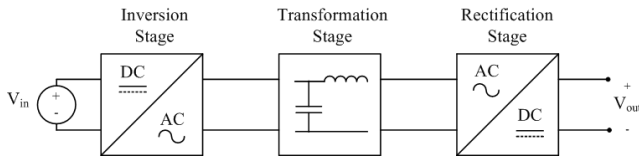


Fig. 1. Architecture of proposed dc/dc converter.

transformer, and a resistance compression network (RCN). The matching network acts as a filter and provides a voltage gain [10], hence reducing the transformer turns ratio requirement. One issue with high-turns-ratio step-up transformers that exists in many topologies is that the parasitic leakage inductance of the transformer can undesirably ring with its secondary side winding capacitance at the switching transitions. This creates large ringing in the current and voltage waveforms, and high-frequency losses. The matching network also eliminates this ringing by absorbing the transformer parasitics. The 1:N transformer provides additional voltage gain and isolation. The resistance compression network (composed of L_s and C_s) [8], [9], limits the output power in a desirable manner as the input and output voltages vary. The RCN also includes a series resonant tank (composed of L_r and C_r) [4]. Its purpose is to provide additional filtering. The inversion stage is simply a full-bridge inverter (composed of switches $S_1 - S_4$). A full-bridge is used instead of a half-bridge to reduce the voltage gain requirement from the matching network and the transformer. The rectification stage is composed of two half-bridge rectifiers. The half-bridge rectifiers provide an additional gain of two relative to full-bridge rectifiers, hence also reducing the gain requirement from the transformation stage. The capacitors C_i and C_o are for input and output filtering, respectively, and the two capacitors marked as C_{DC} are for dc blocking purposes.

The output power in the proposed converter is regulated using on-off control, also known as burst-mode control or bang-bang control. Power is controlled by gating the converter on and off at a modulation frequency that is much lower than the switching frequency [2], [11]. The advantage of using on-off control is that the magnetics are designed for only a single frequency (a high frequency) while the power is regulated by

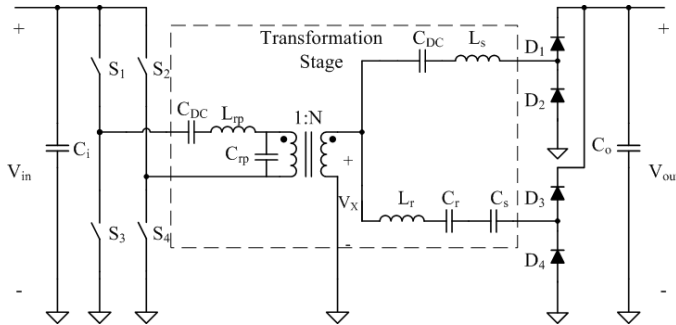


Fig. 2. Topology of the proposed Resistance Compression Network (RCN) converter.

turning the devices on and off at a lower frequency. Moreover, the power is transferred only in the fraction of the time the converter is on, which results in high efficiency even at light loads. The output power is controlled by the duty ratio of the on-off modulation. The on-off modulation has its own corresponding loss. The higher the modulation frequency the greater the loss. The output capacitance is sized according to the modulation frequency. With a lower modulation frequency a larger capacitor has to be used. The duty ratio of the modulation also determines the loss. Very small or very large duty ratio results in greater loss as the converter operates in steady state for a shorter time. So, in order to minimize the total loss both the modulation frequency and the duty ratio have to be considered.

III. ANALYSIS AND DESIGN METHODOLOGY

Using fundamental frequency analysis, at the switching frequency the half-bridge rectifiers can be modeled as resistors [9], as illustrated in Fig. 3. The effective resistance of these rectifiers is given by:

$$R_L = \frac{4V_{out}^2}{\pi^2 P_{out}}, \quad (1)$$

where V_{out} is the converter output voltage and P_{out} is the switching-cycle-average output power. One of the legs of the RCN also has a series resonant tank tuned to the switching frequency. Since, the tank appears as a short circuit at the switching frequency, it is treated as such in Fig. 3 and in the following analysis. Similarly the dc blocking capacitor C_{DC} of Fig. 2 is an effective short at the high switching frequency. Hence, at the switching frequency the input impedance of the RCN looks purely resistive and is given by:

$$Z_{RCN} = \frac{X_s^2 + R_L^2}{2R_L}, \quad (2)$$

where X_s is the magnitude of impedance of the RCN elements (L_s and C_s) at the switching frequency. The use of the resistance compression network reduces the change in impedance seen by the inverter as the effective rectifier resistance (R_L) changes due to variations in output voltage and output power [8], [9]. This compression effect can be seen in Fig. 4, which shows that the RCN input impedance (Z_{RCN}) varies only by

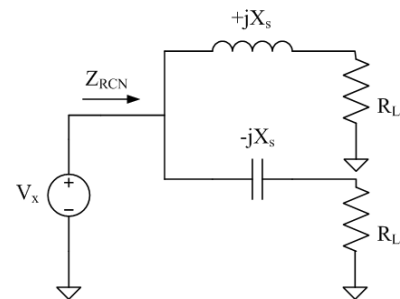


Fig. 3. Fundamental frequency model of the resistance compression network (RCN) and the rectifiers.

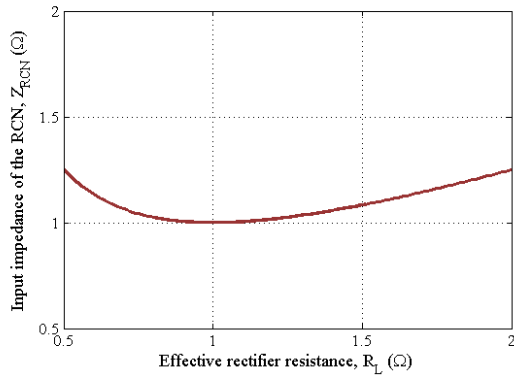


Fig. 4. Variation in the input impedance of the resistance compression network (Z_{RCN}) as a function of the effective rectifier resistance (R_L). Z_{RCN} is plotted assuming the reactance X_s has a value of 1Ω .

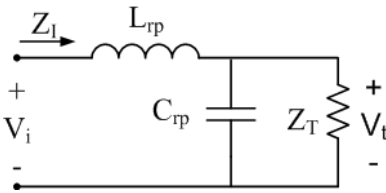


Fig. 5. Matching network with equivalent impedance.

25% while the effective rectifier resistance varies by 400%. This helps achieve zero voltage switching (ZVS) and near zero current switching (ZCS) of the inverter switches across a wide range of output and input voltages. The RCN also serves to limit the instantaneous output power across the full operating range by providing a specified loading characteristic. The value of X_s is selected in such a way so as to limit the output power to the maximum value required at the minimum input voltage. Since the power delivery capability of the converter increases with input voltage, this ensures that the converter can deliver the maximum required power across its entire input voltage range. The expression for output power (P_{out}) can be found by neglecting losses and equating input power ($P_{in} = (\frac{4}{\pi} V_{in})^2 / 2Z_i$, where Z_i is the input impedance of the matching network as shown in Fig. 5) to output power ($P_{out} = 4V_{out}^2 / \pi^2 R_L$). The output power of the converter is given by:

$$P_{out} = \frac{4V_{out}}{X_s \pi^2} \sqrt{4V_{in}^2 N^2 G^2 - V_{out}^2} \quad (3)$$

This expression for output power is in terms of input voltage (V_{in}), output voltage (V_{out}), the transformer turns ratio (N) and the matching network gain voltage (G).

The gain of the matching network can be calculated using the equivalent circuit of Fig. 5 and is given by:

$$G \equiv \frac{V_t}{V_i} = \frac{1}{\sqrt{(c \frac{\omega L_{tp}}{Z_T})^2 + (1 - \omega^2 L_{tp} C_{rp})^2}} \quad (4)$$

where ω is the angular switching frequency. Here Z_T

($=Z_{RCN}/N^2$) is the effective load seen by the matching network. As Z_T varies with changes in power, the gain varies. However, due to the resistance compression network, this gain is fairly constant across variation in input and output voltage. The input impedance of the matching network as seen by the inverter is given by:

$$Z_I = \frac{j(X_{Lrp} Z_T^2 + X_{Crp}^2 X_{Lrp} - X_{Crp} Z_T^2) + X_{Crp}^2 Z_T}{Z_T^2 + X_{Crp}^2} \quad (5)$$

where X_{Lrp} and X_{Crp} are the magnitude of the impedance of L_{rp} and C_{rp} , respectively. For Z_I to be resistive X_{Lrp} , X_{Crp} and Z_T must satisfy:

$$X_{Lrp} = \frac{X_{Crp} Z_T^2}{X_{Crp}^2 + Z_T^2} \quad (6)$$

Picking X_{Lrp} to be slightly larger than the value given by (6), so that Z_I is slightly inductive, ensures that the inverter switches achieve zero voltage switching (ZVS) and near zero current switching (ZCS). The equations presented above are used in the design of the prototype converter in the next section.

IV. PROTOTYPE CONVERTER DESIGN

A prototype of the RCN dc/dc converter of Fig. 2 has been designed and built. The designed dc/dc converter is meant to be part of a two-stage photovoltaic-to-grid conversion system, as shown in Fig. 6. The RCN dc/dc converter is designed to convert the low (widely varying) output voltage of a photovoltaic panel into a high dc-link voltage. The design specifications for this prototype are given in Table I. The converter is required to operate over an input voltage range of 25-40 V, at an output voltage range of 250-400 V and over a wide output power range of 20-200 W.

The switching frequency of the converter is chosen to be 500 kHz, and the on/off modulation frequency for output power control is chosen to be 500 Hz. The components used in the inversion, transformation and rectification stage of the converter are listed in Table II. For the full-bridge inverter, EPC 100-V/25-A enhancement mode GaN transistors (EPC2001) were used. Two of these devices were paralleled for each switch to reduce the conduction loss. Two half-bridge gate drivers for enhancement mode GaN FETs (LM5113) have been chosen. This is a 5-A/100-V bridge driver with an integrated high-side bootstrap diode. It also has under-voltage lockout capability. The transistors are switched at 500 kHz using TI's digital signal controller (TMS320F28335). This has PWM modules that can easily be programmed to produce the required waveforms with a minimum of 10 ns dead time. For the rectifier, silicon carbide Schottky diodes (C3D02060E) were used. These are 2 A devices with 600 V blocking capability.

For the transformation stage, the reactive elements values were chosen considering the trade-offs between the losses in the parasitics of the transformer, the matching network and the RCN. If the total gain provided by the transformer and matching network is increased, the magnitude of impedance

TABLE I
DESIGN SPECIFICATIONS FOR THE PROTOTYPE CONVERTER.

Parameter	Value
Input Voltage (V_{in}) Range	25 V - 40 V
Output Voltage (V_{out}) Range	250 V - 400 V
Output Power (P_{out}) Range	20 W - 200 W

of the RCN also has to be increased. This helps in reducing the increase in output power at higher output voltages, which in turn helps maintain high efficiencies at the higher output voltages. If more gain is provided by the matching network, the value of the matching network inductance needed increases and the losses in this inductance also increase. However, this results in a decrease in the required gain of the transformer leading to a decrease in the number of its secondary turns. Hence, the winding loss in the transformer decreases. On the other hand, the volts-seconds at the transformer primary increase thus increasing the core loss. An analysis of these losses was carried out to find the optimal values for the reactive elements. This optimization showed that the transformer turns ratio (N) should be 6 and the gain of the matching network (G) should be 1.67, for a total gain of approximately 10.

The value of X_s was calculated using (3) with the output power set to its maximum value of 200 W and input voltage set to its minimum value of 25 V and output voltage set to 400 V. From this the value of L_s and C_s were obtained using $L_s = X_s / \omega$ and $C_s = 1 / \omega X_s$. The values of L_{rp} and C_{rp} were calculated using (4) and (6) which makes the input impedance of the matching network resistive. However, the value of L_{rp} was increased slightly to provide slightly inductive loading of the inverter to achieve ZVS switching of the inverter switches.

For the design of the magnetic structure, a trade-off was made between loss and size. For the transformer and inductors, different core sizes (RM10, RM12 and RM14) and types of windings (litz wire and foil) were considered. For the transformer, RM12 provided a good balance between loss and size. Copper foil was chosen for the primary winding due to the high current and litz wire was chosen for the secondary winding to reduce the proximity effect given the large number of turns. For the inductors (L_s , L_r and L_{rp}), RM12 core and litz wire were chosen. Mica capacitors were used for C_s and C_r due to their stable capacitance value characteristics. The design value for C_s was 1300 pF and for C_r was 1000 pF. However, since these were in series, a single capacitor of 560 pF was used instead. Six 10 nF ceramic capacitors with

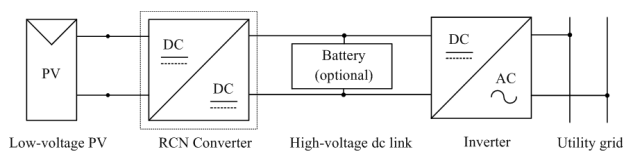


Fig. 6. Block diagram of a grid-connected PV system.

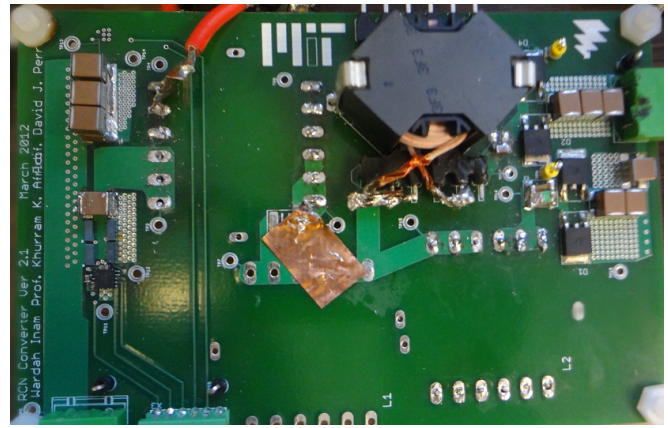


Fig. 7. Photograph of the prototype RCN dc/dc converter.

TABLE II
COMPONENTS USED IN THE EXPERIMENTAL PROTOTYPE.

Components	Type
Transistors	100-V/25-A GaN enhancement mode power transistor (EPC's EPC2001), Qty: 8 (2 in parallel per switch)
Drivers	100-V/5-A half-bridge gate driver for enhancement mode GaN FETs (TI's LM5113), Qty: 2
Controller	150 MHz digital signal controller (TI's TMS320F28335), Qty: 1
Diodes	600-V/2-A SiC Schottky diode (CREE's C3D02060E), Qty: 4
Transformer	RM12 3F3 core, Copper foil (4 turns, 5 mils width, 3 mils thickness, 3 foils in parallel) and litz wire (24 turns, 46 AWG, 450 strands in parallel)
Capacitors	$C_s + C_r$: 560 pF/1000-V Mica capacitor (C_s :1300 pF and C_r :1000 pF) C_{rp} : 60 nF Ceramic capacitors, Qty: 6 (10 nF capacitors in parallel)
Inductors	L_{rp} : 1 μ H, RM12A115 3F3 core, litz wire (3 turns, 46AWG, 3600 strands in parallel), L_s : 78 μ H, RM12A080 3F3 core, litz wire (31 turns, 46AWG, 450 strands in Parallel), L_r : 101 μ H, RM12A060 3F3 core, litz wire (41 turns, 46AWG, 450 strands in parallel)

very low equivalent series resistance (ESR) were used for C_{rp} . Further design details of this converter are given in [12]. A photograph of the prototype converter is shown in Fig. 7.

V. EXPERIMENTAL RESULTS

The prototype RCN dc/dc converter has been tested using a dc power supply and a resistive load. The tests were carried out with different input voltages (in the 25-40 V range) and different output voltages (in the 250-400 V range). Figure 8 shows current and voltage waveforms for the converter over two switching periods, when operated at an input voltage of 25 V. In particular, it shows the current through the inductor of the matching network, which is also the output current of the inverter, the gate drive voltages of the inverter switches S_1 and S_3 , and the drain-source voltage of the switch S_3 . As expected the current through the inductor of the matching network

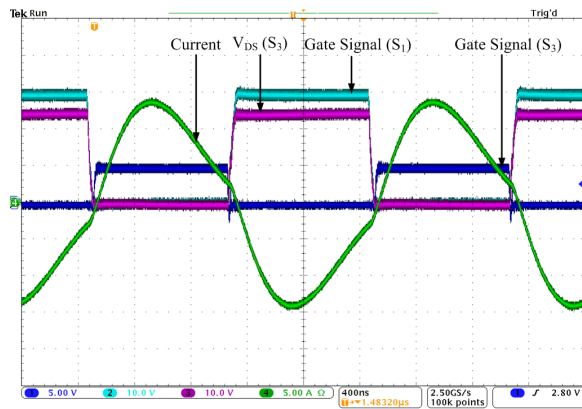


Fig. 8. Current and voltage waveforms of the RCN dc/dc converter when operated at an input voltage of 25 V: (1-blue) Gate voltage of switch S_3 , (2-turquoise) Gate voltage of switch S_1 , (3-magenta) Drain-source voltage of switch S_3 and (4-green) Input current of the parallel tank.

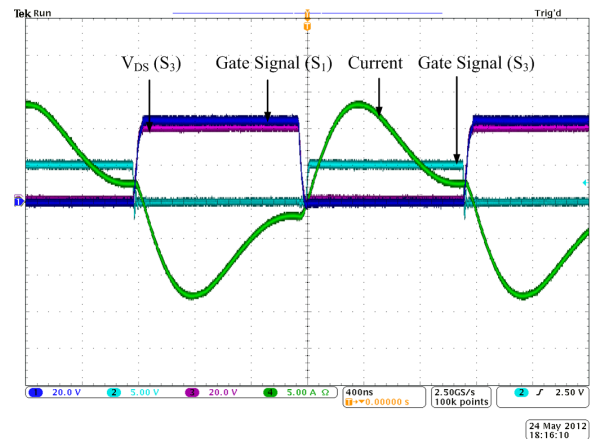


Fig. 10. Current and voltage waveforms of the RCN dc/dc converter when operated at an input voltage of 25 V: (1-blue) Gate voltage of switch S_1 , (2-turquoise) Gate voltage of switch S_3 , (3-magenta) Drain-source voltage of switch S_3 and (4-green) Input current of the parallel tank.

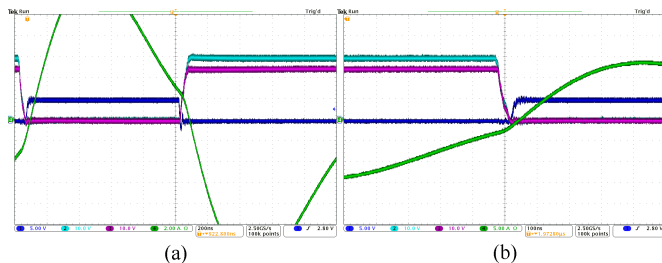


Fig. 9. Current and voltage waveforms of the RCN dc/dc converter when operated at an input voltage of 25 V, showing (a) turn-off transition and (b) turn-on transition. (1-blue) Gate voltage of switch S_3 , (2-turquoise) Gate voltage of switch S_1 , (3-magenta) Drain-source voltage of switch S_3 and (4-green) Input current of the parallel tank.

is nearly sinusoidal. Also the switches achieve zero voltage switching (ZVS) and near zero current switching (ZCS), as can be seen from Fig. 9. Figure 9(a) shows a zoomed in view of the turn-off transition of switch S_3 . The current through switch S_3 at turn-off is very small compared to the peak current it carries (turn-off current is 15.7% of peak current). Figure 9(b) shows the turn-on transition of switch S_3 . Notice that the switch turns-on under ZVS, as the voltage across the switch falls to zero before the switch is turned on. Figure 10 shows the current and voltage waveforms with an input voltage of 40 V and an output voltage of 400 V. The converter was operated off resonance at 425 kHz switching frequency to decrease the maximum output power at the increased input voltage. This off resonance operation results in a slight distortion of the current waveform as can be seen in Fig. 10. However, this converter still maintains ZVS and near ZCS operation.

The converter maintains near ZCS operation over the entire input voltage and output voltage range. The highest current at switch turn-off is no more than 13.6% of peak switch current when the converter is operated at its nominal input voltage of 32.5 V. When the input voltage is at its minimum of 25 V, the switch turn-off current is still only 15.7% of peak switch current; and when the input voltage is at its maximum of 40 V,

the switch turn-off current rises to only 18.9% of peak switch current.

By adjusting the converter switching frequency over a narrow range from 425 kHz to 500 kHz, the maximum output power that can be delivered by the converter can be maintained within limits across variations in input voltage. This helps maintain high efficiency as the input voltage varies. The switching frequency needs to be increased as the input voltage decreases: 500 kHz is used at an input voltage of 25 V and 425 kHz with an input voltage of 40 V. The maximum output power then varies from 200 W to 325 W across the full range of input voltage, with the output voltage at 400 V, as shown in Fig. 11(a). The converter was also tested for output voltage variations from 250 V to 400 V. When the output voltage is reduced from 400 V to 250 V with input voltage held at 25 V (and switching frequency held constant), the maximum output power drops slightly from 203 W to 195 W, as shown in Fig. 11(b).

The efficiency of the RCN dc/dc converter was also measured across variations in input voltage, output voltage and output power. The measured efficiency of the converter as a function of input voltage is plotted in Fig. 12. The converter maintains efficiency above 95% across the full range of input voltage. The efficiency of the converter increases from 95% to 95.6% as input voltage increases from 25 V to 40 V. The efficiency of the converter as a function of output voltage is shown in Fig. 13. As the output voltage decreases from 400 V to 250 V, with input voltage held constant at 25 V, the efficiency of the converter drops from 95% to 93.7%. The lower efficiency at the lower output voltage is due to the larger currents flowing through the output stages of the converter.

The output power of the converter is controlled below its maximum value using on/off control at an on/off modulation frequency of 500 Hz. The output power is determined by the duty ratio of modulating waveform. A 100% duty ratio delivers maximum power (roughly 200 W at 25 V) and a 10% duty

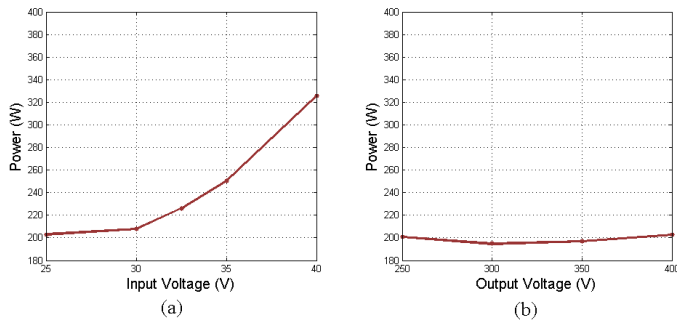


Fig. 11. Output power of the RCN dc/dc converter with (a) input voltage variation and (b) output voltage variation.

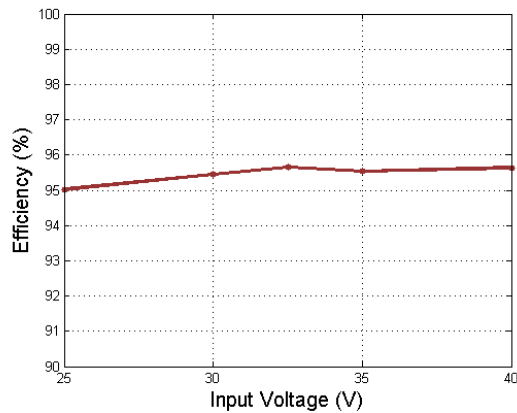


Fig. 12. Efficiency of the RCN dc/dc converter as the input voltage varies.

ratio corresponds to 10% of maximum power (roughly 20 W at 25 V). The efficiency of the converter as a function of output power is shown in Fig. 14. With input voltage of 25 V and output voltage of 400 V, the efficiency varies from 95% to 93.4% as output power is reduced from full load (200 W) to 10% of full load (20 W). These results demonstrate that the proposed RCN dc/dc converter can maintain ZVS and near ZCS operation and offer high efficiency across a wide input voltage, output voltage and output power range.

VI. CONCLUSION

This paper presents a new resonant dc/dc converter topology that uses a resistance compression network and a combination of on/off control and narrowband frequency control. The converter implementation provides galvanic isolation and enables large (greater than 1:10) voltage conversion ratios. The proposed converter overcomes the challenges faced by many previously reported resonant converters, and achieves very high efficiency by maintaining ZVS and near ZCS over a wide input voltage, output voltage and power range. The experimental results from a 200 W prototype show that the converter maintains an efficiency of over 95% across its entire 25-40 V input voltage range at the designed output voltage of 400 V; an efficiency of over 93.7% as output voltage is reduced down to 250 V; and an efficiency of over 93.4% even

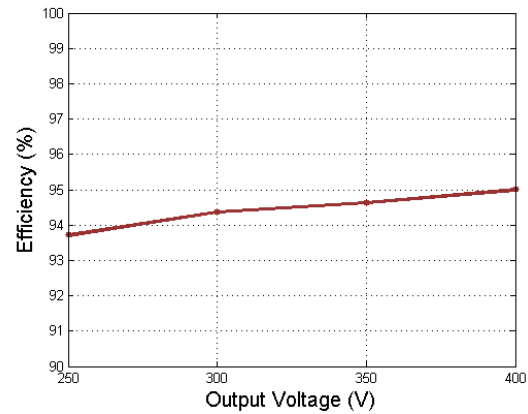


Fig. 13. Efficiency of the RCN dc/dc converter as the output voltage varies.

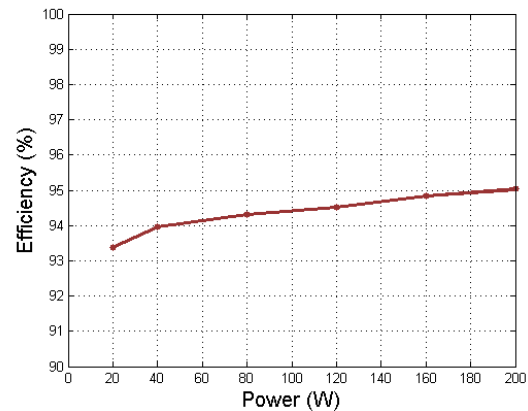


Fig. 14. Efficiency of the RCN dc/dc converter as the output power is varied using on/off control. This was measured with $V_{in} = 25$ V and $V_{out} = 400$ V.

as output power is reduced to 20 W. This demonstrates the effectiveness of the approach.

ACKNOWLEDGMENT

The authors wish to acknowledge the financial support received from Masdar Institute for this project.

REFERENCES

- [1] J. S. Lai, "Power Conditioning Circuit Topologies," *IEEE Industrial Electronics Magazine*, pp. 24-34, June 2009.
- [2] Q. Li and P. Wolfs, "A Review of the Single-Phase Photovoltaic Module Integrated Converter Topologies with Three Different DC Link Configurations," *IEEE Transactions on Power Electronics*, vol. 23, no. 3, pp. 1320-1333, May 2008.
- [3] R. L. Steigerwald, "High-Frequency Resonant Transistor DC-DC Converters," *IEEE Transactions on Industrial Electronics*, vol. IE-31, no. 2, pp. 181-191, May 1984.
- [4] R. L. Steigerwald, "A Comparison of Half-Bridge Resonant Converter Topologies," *IEEE Transactions on Power Electronics*, vol. 3, no. 2, pp. 174-182, April 1988.
- [5] J. P. Vandelac and P. D. Ziogas, "A DC to DC PWM Series Resonant Converter Operated at Resonant Frequency," *IEEE Transactions on Industrial Electronics*, vol. 35, no. 3, pp. 451-460, August 1988.
- [6] P. K. Jain, A. St-Martin and G. Edwards, "Asymmetrical Pulse-Width-Modulated Resonant DC/DC Converter Topologies," *IEEE Transactions on Power Electronics*, vol. 11, no. 3, pp. 413-422, May 1996.

- [7] Y. S. Lee and Y. C. Cheng, "A 580 kHz Switching Regulator Using On-Off Control," *Journal of the Institution of Electronic and Radio Engineers*, vol. 57, no. 5, pp. 221-226, September-October 1987.
- [8] Y. Han, O. Leitermann, D. A. Jackson, J. M. Rivas, and D. J. Perreault, "Resistance Compression Networks for Radio-Frequency Power Conversion," *IEEE Transactions on Power Electronics*, Vol. 22, No.1, pp. 41-53, Jan. 2007.
- [9] P. A. Godoy, D. J. Perreault and J. L. Dawson, "Outphasing Energy Recovery Amplifier With Resistance Compression for Improved Efficiency," *IEEE Transactions on Microwave Theory and Techniques*, vol. 57, no. 12, pp. 2895-2906, December 2009.
- [10] Y. Han and D. J. Perreault, "Analysis and Design of High Efficiency Matching Networks," *IEEE Transactions on Power Electronics*, vol. 21, no. 5, pp. 1484-1491, September 2006.
- [11] J. Hu, A. D. Sagneri, J. M. Rivas, Y. Han, S. M. Davis, and D. J. Perreault, "High-Frequency Resonant SEPIC Converter with Wide Input and Output Voltage Ranges," *IEEE Transactions on Power Electronics*, Vol. 27, No. 1, pp. 189-200, Jan. 2012
- [12] W. Inam, *High Efficiency Resonant dc/dc Converter for Solar Power Applications*, SM Thesis, Dept. of EECS, Massachusetts Institute of Technology, Cambridge, MA, Feb. 2013.